*Fourth Asia-Pacific Conference on FRP in Structures (APFIS 2013)*
*11-13 December 2013, Melbourne, Australia*


# REDUCTION OF THERMAL STRESS INDUCED IN STEEL PLATE STRENGTHENED BY BONDING CFRP PLATE ON ONE SIDE

T. Ishikawa [1], T. Nagao [2], A. Kobayashi [3], M. Shimizu [4], A. Hattori [5] and H. Kawano [6]
[1] Department of Urban Management,
Kyoto University, Japan. Email: ishikawa.toshiyuki.2e@kyoto-u.ac.jp
[2] Nippon Light Metal Co., Ltd., Shizuoka, Japan, takashi-nagao@nikkeikin.co.jp
[3] Nippon Steel Materials Co., Ltd., Tokyo, Japan, a-kobayashi@nck.nsmat.co.jp
[4] Department of Urban Management,
Kyoto University, Japan. Email: shimizu.masaru.75w@st.kyoto-u.ac.jp
[5] Department of Urban Management,
Kyoto University, Japan. Email: hattori.atsushi.7z@kyoto-u.ac.jp
[6] Department of Urban Management,
Kyoto University, Japan. Email: kawano.hirotaka.8n@kyoto-u.ac.jp

## ABSTRACT

In steel members strengthening with CFRP plate, thermal stress is introduced in steel members by temperature change, due to the mismatch of coefficients of linear thermal expansion of steel and CFRP. In the previous study, a reduction technique of thermal stress in steel members, which is additional bonding of aluminum alloy plates with CFRP plates, was proposed. However, by bonding laminated plate consisting of CFRP and aluminum plates on one side of thin steel plate, thermal stress is not completely reduced. Therefore, to confirm the effectiveness of proposed method for one side bonding, heat tests of steel plate with bonding laminated plate on one side were carried out. Additionally, to verify the test results, numerical analysis for proposed method was also carried out. As a result, it was found that the three-layered laminated plate consisting of one CFRP plate and two aluminum plates was required for reduction of thermal stress in thin steel plate.

## KEYWORDS

CFRP, aluminum alloy, steel plate, strengthening, thermal stress.

## INTRODUCTION

Recently, carbon fiber reinforced polymer, CFRP, plates have been used for the strengthening or rehabilitation of steel structures (Miller *et al.* 2001; Tamai *et al*. 2005; Moy and Bloodworth 2007 and Täljsten *et al*. 2009). CFRP plate has an excellent material properties with low weight, and the application of CFRP plate brings the rapid repair works.
Typical linear thermal expansion coefficients of steel and CFRP plate are listed Table 1. As can be seen in this table, coefficients of linear thermal expansion of CFRP plate is almost zero. Therefore, when the temperature is changed, the thermal stress is introduced in steel member strengthened with bonding CFRP plates by mismatch of the thermal expansions of steel and CFRP. Accordingly, thermal stress is considered in the design of strengthening or rehabilitation of steel members with bonding CFRP plate (Schnerch *et al.* 2007; National Research Council 2007).

Table 1 Comparison of coefficients of linear thermal expansion of steel, CFRP and aluminum alloy

| Materials | Coefficients of linear thermal expansion [μ/°C ] |
|---|---|
| Steel | 11.5-12.0 |
| CFRP plate | 0-1.0 |
| Aluminum alloy | 21.0-24.0 |

In the previous study, a reduction technique of thermal stress in steel members, which is additional bonding of aluminum alloy plates with CFRP plates, was proposed (Ishikawa *et al.* 2011, 2012). The linear thermal expansion coefficient of aluminum alloy is about twice higher than that of steel, as listed in Table 1. Therefore,

the coefficient of linear thermal expansion of laminated plate consisting of CFRP and aluminum plates can be corresponding to that of steel. The thermal stress in steel plate with laminated plate is also able to control as zero. However, by bonding laminated plate consisting of CFRP and aluminum plates on one side of thin steel plate, thermal stress is not completely reduced. This is because the thermal bending moment is caused by mismatch of the distances from the centroid of the composite member to each plate, as shown in Fig.1.
In this study, to confirm the effectiveness of proposed method for one side bonding, heat tests of steel plates with bonding laminated plate on one side are carried out. Additionally, to verify the test results, a numerical analysis of laminated plates bonded onto steel member is proposed and carried out.

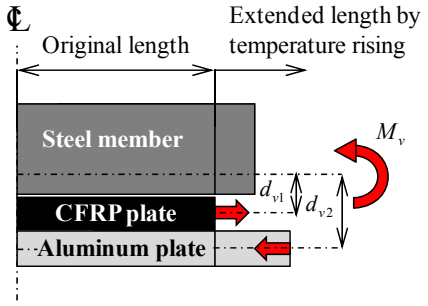


Figure 1. Bending moment introduced in composite member by temperature change

## SPECIMEN AND HEAT TEST

### Laminated plate

Generally, the coefficient of linear thermal expansion of CFRP plates can be easily controlled by volume fraction of carbon fibers. However, if the linear thermal expansion coefficient of CFRP plate is controlled as 11.7μ/°C, Young's modulus of CFRP plate becomes almost the same as that of matrix resin because of the low volume fraction of carbon fibers. Therefore, to reduce the thermal stress in steel structures strengthened by CFRP plates, the authors have proposed the additional bonding of aluminum plates, which has relatively higher coefficient of linear thermal expansion and Young's modulus (Ishikawa *et al.* 2011, 2012).
The linear thermal expansion coefficient of CFRP and aluminum laminated plate, $\alpha_v$, can be calculated by:

$$\alpha_v = \frac{\alpha_f E_f A_f + \alpha_a E_a A_a}{E_f A_f + E_a A_a} \tag{1}$$

where, $E_f$ and $E_a$ denote the Young's modulus of CFRP and aluminum plates, respectively, $A_f$ and $A_a$ are the cross-sectional areas of CFRP and aluminum plates, respectively, $\alpha_f$ and $\alpha_a$ are the linear thermal expansion coefficient of CFRP and aluminum plates, respectively.
By substituting the linear thermal expansion coefficient of steel, $\alpha_s$, into $\alpha_v$, the stiffness ratio, $E_a A_a / (E_f A_f)$, is given by:

$$\frac{E_a A_a}{E_f A_f} = \frac{\alpha_s - \alpha_f}{\alpha_a - \alpha_s} \tag{2}$$

Accordingly, to design the linear thermal expansion coefficient of laminated plate as same as that of steel, the required stiffness of aluminum plate can be given by Eq. (2).
Therefore, the cross-sectional areas of CFRP and aluminum plates for proposed method are respectively given by:

$$A_f = \frac{\alpha_a - \alpha_s}{\alpha_a - \alpha_f} A_{f0} \tag{3}$$

$$A_a = \frac{E_f}{E_a} \cdot \frac{\alpha_s - \alpha_f}{\alpha_a - \alpha_s} A_{f0} \tag{4}$$

where, $A_{f0}$ is the required cross-sectional area of CFRP plats in conventional CFRP bonding method.

### Material property

The material properties given by the coupon tests are listed in Table 2. The steel plates used in this study are the JIS SS400 (guaranteed yield stress of 245N/mm$^2$) or JIS SM490Y (guaranteed yield stress of 365N/mm$^2$). CFRP plate is fabricated by pultrusion technique. The aluminum alloy plate of AA5052 is used in this study.

Table 2 Material properties

(a) Steel plates

| Steel type | SS400 | SM490Y |
|---|---|---|
| Thickness $t_s$ | 4.4 | 11.6 |
| $\alpha_s$ [μ/°C] | 10.5 | 11.0 |
| $E_s$ [GPa] | 210 | 202 |
| Yield stress $\sigma_Y$ [MPa] | 335 | 393 |
| Tensile strength [MPa] | 330 | 391 |
| Poisson's ratio | 445 | 548 |
| Elongation [%] | 0.29 | 0.29 |

(b) CFRP plate

| | |
|---|---|
| Thickness $t_f$ | 1.0 |
| $\alpha_f$ [μ/°C ] | 0.8 |
| $E_f$ [GPa] | 141 |
| Tensile strength [MPa] | 2801 |

(c) Adhesive

| | |
|---|---|
| Glass transition [°C] | 74.0* |
| Working life [minutes] | 37* |
| Tensile shear strength [MPa] | 23.8* |
| Young's modulus [GP] | 2.61*, 1.60 |
| Poisson's ratio | 0.35 |

* given by the mill test report

(d) Aluminum alloy plate (AA5052)

| Thickness $t_a$ | 1.0 | 2.0 |
|---|---|---|
| $\alpha_a$ [μ/°C] | 21.4 | 21.4 |
| $E_a$ [GPa] | 70.0 | 69.7 |
| $\sigma_{0.2}$ [MPa] | 227 | 190 |
| Tensile strength [MPa] | 283 | 252 |
| Poisson's ratio | 0.33 | 0.33 |
| Elongation [%] | 8.3 | 10.7 |

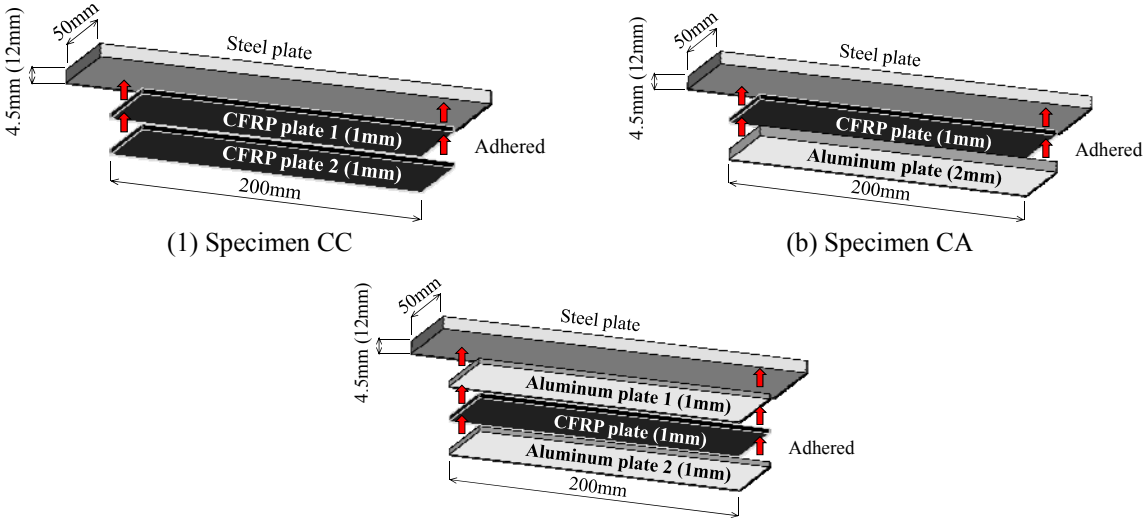


Figure 2. Test specimens

**Specimens**

The specimens used in this research are shown in Fig.2. Specimen CC is the conventional CFRP bonded steel plate. Two layer of CFRP plates of 1mm in thickness are used. Therefore, the cross-sectional area of the conventional CFRP bonding method, $A_{f0}$, is 100mm$^2$. In the specimen CA, a proposed laminated plate consisted of CFRP and aluminum plates is adhered on one side of the steel plate. The thickness of CFRP plate in specimen CA is 1mm, which is calculated from Eq.(3) by substituting the material properties of CFRP and aluminum plates. The thickness of aluminum plate in spceimen CA is 2mm, which is calculated from Eq.(4). In the specimen ACA, a laminated plate consisted of one CFRP and two aluminum plates is used. In specimen ACA, the thickness of each aluminum plate is 1mm which is the half thickness of aluminum plate in specimen CA.
The bond surfaces of steel, CFRP and aluminum plates were sandpapered with #100 abrasive paper specified in JIS R611. All the specimens were cured one week in the temperature controlled room in 20°C. The measured thicknesses of average adhesive layers are also listed in Table 3.
The locations of strain gages are illustrated in Fig.3.

Table 3 Average adhesive thickness [mm]

| Specimen | CC | CA | ACA | $\Delta T$ [°C] |
|---|---|---|---|---|
| Steel plate of 4.5mm thickness | 0.28 | 0.38 | 0.36 | 23.4 |
| Steel plate of 12mm thickness | 0.24 | 0.29 | 0.27 | 22.5 |

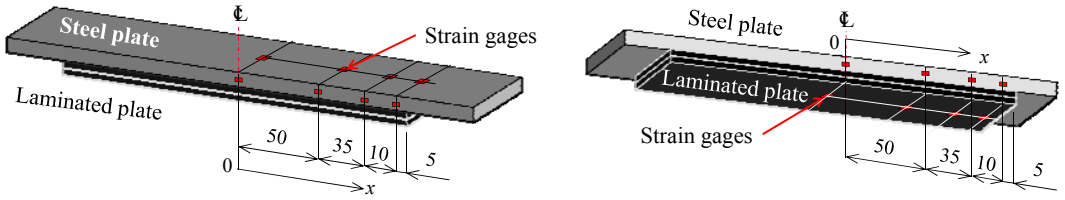


Figure 3. Locations of strain gages

**Heat test**

Heat tests were carried out using electric oven. Initial and maximum temperatures were controlled as 20°C and 40°C, respectively. The measured temperatures are listed in Table 3.
To confirm the coefficient of linear thermal expansion of materials as well as to calculate the thermal stresses in specimens, the strains of free expansion in steel, CFRP and aluminum plates were also measured.
By using measured strains, thermal stresses in steel plates, CFRP and aluminum plates were respectively calculated by the following equations.

$$\sigma_s = E_s(\varepsilon_{sm} - \varepsilon_{sf}) \tag{5}$$

$$\sigma_f = E_f(\varepsilon_{fm} - \varepsilon_{ff}) \tag{6}$$

$$\sigma_a = E_a(\varepsilon_{am} - \varepsilon_{af}) \tag{7}$$

where, $\varepsilon_{sm}$, $\varepsilon_{fm}$ and $\varepsilon_{am}$ are the measured strains of steel, CFRP and aluminum plates in specimens, respectively, and $\varepsilon_{sf}$, $\varepsilon_{ff}$ and $\varepsilon_{af}$ are the free expand strains of steel, CFRP and aluminum plates, respectively.

## CALCULATION OF THERMAL STRESS

**Composite theory**

By using composite theory to the laminated plate bonded on one side of the steel plate, the thermal stresses introduced in steel, CFRP and aluminum plates are calculated by:

$$\sigma_s = \frac{M_v}{I_v} y_{vs} + \frac{P_v}{A_v} \tag{8}$$

$$\sigma_i = \frac{1}{n_i}\left(\frac{M_v}{I_v} y_{vs} + \frac{P_v}{A_v}\right) - \frac{P_i'}{A_i} \tag{9}$$

where,

$$P_v = \sum P_i' \tag{10}$$

$$M_v = \sum (P_i' \cdot d_{vi}) \tag{11}$$

$$P_i' = E_i A_i (\alpha_i - \alpha_s)\Delta T \tag{12}$$

$$n_i = E_s / E_i \tag{13}$$

$I_v$, $A_v$ and $y_{vs}$ are the moment of inertia of the composite member, cross-sectional area of composite member and the distance from the centroid of the composite member, respectively, $d_{vi}$ is the distance between centroid in the composite member and that in the attached plate $i$, $E_i$, $A_i$, $\alpha_i$ are the Young's modulus, the cross-sectional area and the linear thermal expansion coefficient of plate $i$, respectively and $\Delta T$ is the temperature range in which the positive value means the temperature rising.

**Numerical analysis method**

The thermal stress induced in composite member calculated by Eqs.(8) and (9) are the constant value through the longitudinal direction of the members. However, the shear transfer lag is observed between steel and CFRP

plates as well as between CFRP and aluminum plates. Therefore, thermal stresses in composite member are not constant through the longitudinal direction.

Generally, the solution of differential equation derived by the equilibrium of the cross-sectional forces of the differential segment gives the stress distribution including the shear lag effects. However, the solution of multi layer plates bonded onto steel member have not been mathematically solved. Thereby, to clarify the distribution of thermal stresses in composite members, simple numerical analysis method is proposed.

The numerical analysis can calculate the shear and normal stresses in adhesive with adopting the following three assumptions:

(1) the materials are all linearly elastic;

(2) the shear and normal stresses in the adhesive layer are constant through the thickness;

(3) the axial force, shear force, and bending moment in the adhesive are negligible because of the low elasticity of the adhesive.

The shear and normal stresses are assumed in the numerical analysis by the following equations.

$$\tau_{ei}(x) = G_{ei}\frac{u_{i-1,L}(x) - u_{i,U}(x)}{h_i} \tag{14}$$

$$\sigma_{yei}(x) = E_{ei}\frac{v_{i-1}(x) - v_i(x)}{h_i} \tag{15}$$

where, $u_i(x)$ is the horizontal displacement on upper (U) or lower (L) surface of the plate $i$ ($u_{0,L}(x)$ means the horizontal displacement on lower surface of the steel plate), $v_i(x)$ is the vertical displacement of the plate $i$ ($v_0(x)$ means the vertical displacement of steel plate), $G_{ei}$, $E_{ei}$ and $h_i$ are the shear modulus, Young's modulus and the thickness of adhesive layer $i$.

The following first order of multi differential equations of strains are given by the equilibrium of the cross-sectional forces of the differential segment as shown in Fig.4.

$$\frac{d\boldsymbol{\varepsilon}(x)}{dx} = A\boldsymbol{\varepsilon}(x) \tag{16}$$

where

$$\underset{(6N+3)\times 1}{\boldsymbol{\varepsilon}(x)} = \left\{\varepsilon_{Ns}(x)\ \gamma_s(x)\ \varepsilon_{Ms}(x)\ \varepsilon_{N1}(x)\ \gamma_1(x)\ \varepsilon_{M1}(x)\ \varepsilon_{ye1}(x)\ \gamma_{e1}(x)\ \varepsilon_{ye1}'(x)\cdots\varepsilon_{Ni}(x)\ \gamma_i(x)\ \varepsilon_{Mi}(x)\ \varepsilon_{yei}(x)\ \gamma_{ei}(x)\ \varepsilon_{yei}'(x)\cdots\right\}^T \tag{17}$$

$$\underset{9\times 9}{A} = \begin{bmatrix} B_{a0} & B_0 & B_{b1} \\ B_0 & B_{a1} & B_{c1} \\ B_{d1} & B_{e1} & B_1 \end{bmatrix} (N=1),\quad \underset{(6i+3)\times(6i+3)}{A} = \left[\begin{array}{ccc|cc} & \underset{(6i-3)\times(6i-3)}{A} & & B_0 & B_0 \\ & & & \vdots & \vdots \\ & & & B_0 & B_{bi} \\ & & & B_0 & B_0 \\ \hline B_0 & \cdots & B_0\ B_0 & B_{ai} & B_{ci} \\ B_0 & \cdots & B_{di}\ B_0 & B_{ei} & B_1 \end{array}\right] (i = 2 \text{ to } N) \tag{18}$$

$\sigma_{Ns}(x)$, $\varepsilon_{Ns}(x)$, $\tau_s(x)$, $\gamma_s(x)$, $\sigma_{Ms}(x)$ and $\varepsilon_{Ms}(x)$ are respectively the axial stress and strain in steel plate, the shear stress and strain in steel plate, the bending stress and strain at the lower surface of steel plate, $\sigma_{Ni}(x)$,

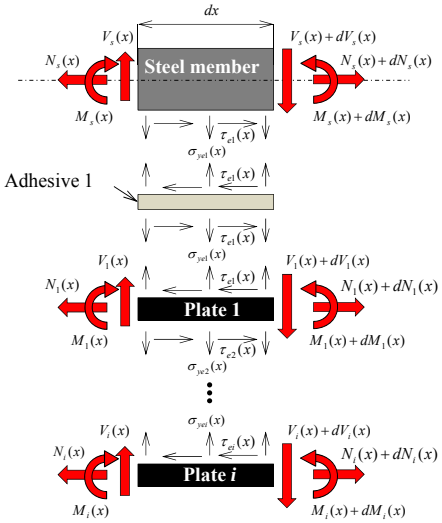


Figure 4. A differential segment of strengthened steel member

$\varepsilon_{Ni}(x)$, $\tau_i(x)$, $\gamma_i(x)$, $\sigma_{Mi}(x)$ and $\varepsilon_{Mi}(x)$ are respectively the axial stress and strain in plate *i*, the shear stress and strain in plate *i*, the bending stress and strain at the lower surface of plate *i*, $\sigma_{yei}(x)$, $\varepsilon_{yei}(x)$, $\tau_{ei}(x)$ and $\gamma_{ei}(x)$ are the normal (peel) stress and strain in adhesive layer *i*, the shear stress and strain in adhesive layer *i*, respectively, and the $\sigma_{yei}'(x)$, $\varepsilon_{yei}'(x)$ are the auxiliary functions which are employed to reduce the dimension of second-order differential equation.

The general solution of Eq.(16) is given by (Miyashita and Nagai 2010);

$$\boldsymbol{\varepsilon}(x) = Y(x)\mathbf{C} \tag{19}$$

where

$$\underset{(6N+3)\times 1}{\mathbf{C}} = \left\{C_1 \quad \cdots \quad C_j\right\}^T \tag{20}$$

$$\underset{(6N+3)\times(6N+3)}{Y(x)} = Te^{\Lambda(x)}T^{-1} \tag{21}$$

$$\underset{(6N+3)\times(6N+3)}{e^{\Lambda(x)}} = \begin{bmatrix} e^{\lambda_1 x} & & 0 \\ & \ddots & \\ 0 & & e^{\lambda_j x} \end{bmatrix} \tag{22}$$

$$\underset{(6N+3)\times(6N+3)}{T} = \left[\mathbf{v}_1 \quad \cdots \quad \mathbf{v}_j\right] \tag{23}$$

$\lambda_j$ is the $j$ th eigenvalue of matrix $A$, $\mathbf{v}_j$ is the $j$ th eigenvector of matrix $A$, $j$ is the integer number of 1 to 6*N*+3 and *N* is the total number of layers in laminated plate.

Unknown coefficient vector, **C**, is given by the boundary conditions and continuous conditions of strains. In this study, unknown coefficient vector, **C**, is calculated by the following equation.

$$\mathbf{C} = H^{-1}\left(\boldsymbol{\varepsilon}_0 + \boldsymbol{\varepsilon}_T\right) \tag{24}$$

where, $H$ consists of the row vector components of matrix $Y(x)$, which applied the boundary conditions and $\boldsymbol{\varepsilon}_0$ is the strain vector of external forces.

$$\underset{(6N+3)\times 1}{\boldsymbol{\varepsilon}_T} = \left\{\alpha_s\Delta T \;\; 0 \;\; 0 \;\; \alpha_1\Delta T \;\; 0 \;\; 0 \;\; 0 \;\; 0 \;\; 0 \cdots \alpha_i\Delta T \;\; 0 \;\; 0 \;\; 0 \;\; 0 \;\; 0 \cdots\right\}^T \tag{25}$$

Furthermore, by substituting $\boldsymbol{\varepsilon}(x)$ given by Eq.(19) into the following equation, thermal stresses in steel plate strengthened with laminated plate are given.

$$\boldsymbol{\sigma}(x) = D\left\{\boldsymbol{\varepsilon}(x) - \boldsymbol{\varepsilon}_T\right\} \tag{26}$$

where,

$$\underset{(6N+3)\times 1}{\boldsymbol{\sigma}(x)} = \left\{\sigma_{Ns}(x)\,\tau_s(x)\,\sigma_{Ms}(x)\,\sigma_{N1}(x)\,\tau_1(x)\,\sigma_{M1}(x)\,\sigma_{ye1}(x)\,\tau_{e1}(x)\,\sigma_{ye1}'(x)\cdots\sigma_{Ni}(x)\,\tau_i(x)\,\sigma_{Mi}(x)\,\sigma_{yei}(x)\,\tau_{ei}(x)\,\sigma_{yei}'(x)\cdots\right\}^T \tag{27}$$

$$\underset{(6N+3)\times(6N+3)}{D} = diag\left\{E_s \;\; G_s \;\; E_s \;\; E_1 \;\; G_1 \;\; E_1 \;\; E_{e1} \;\; G_{e1} \;\; E_{e1} \cdots E_i \;\; G_i \;\; E_i \;\; E_{ei} \;\; G_{ei} \;\; E_{ei} \cdots\right\}^T \tag{28}$$

In this study, the strains vector of the external force, $\boldsymbol{\varepsilon}_0$, is treated as zero, because the objection of this research is to investigate the thermal stress.

## RESULTS AND DISCUSSIONS

### Thermal stresses induced in steel, CFRP and aluminum alloy plates

The thermal stresses induced in the specimens are shown in Figs.5 and 6. In these figures, Y-axis shows the thermal stress and X-axis shows the distance from the centre of the specimen, as shown in Fig.3. In this figure, the thermal stresses calculated by composite theory (dot-dash-line), Eqs.(8) and (9), and the numerical analysis (solid and broken lines), NA, are compared with the test results (open circle). It can be seen that the thermal stresses of composite theory and numerical analysis at *x*=0 in all specimens give results in close agreement with the test results. Additionally, it is clearly seen that the shear lag effect near the attached plate end can be demonstrated by NA.

In specimen CC, the compressive thermal stress by bonding CFRP plates is generated in the lower surface of the steel plate, while the tensile thermal stresses are generated in the upper surface of the steel plate and lower surface of CFRP plates. On the other hand, the thermal stress on upper surface of the steel plate in specimen CA in Figs.5(b) and 6(b) is relatively small, even the tensile thermal stress on lower surface of CFRP plate becomes higher than that in the conventional CFRP bonded specimen CC. Further, in the specimen CA, the thermal stress in steel plate of 12mm in thickness is smaller than that in steel plate of 4.5mm in thickness.

In Figs.5(c) and 6(c), the fairly-low thermal stresses in steel plates are observed in specimen ACA for the both steel thicknesses of 4.5mm and 12mm. This is because the thermal bending moment calculated by Eq.(11) becomes zero when the odd-layers of laminated plate is used.

Therefore, it is clear that the use of laminated plate consisted of CFRP and aluminum plates is effective to reduce the thermal stress in steel plate. Further, for the thin steel plate, the thermal stress in steel plate can be significantly reduced by bonding the odd-layers of laminated plate.

From the temperature test results, it seems that the thermal stress introduced in aluminium plate was relatively small compared with the yielding stress or the buckling stress in aluminium plate under the ordinary temperature environment. However, it should be concern about the stress in aluminum plate, because the stress is also introduced in aluminum plate by loading as well as by temperature change. It is clear from Figs.5(b), (c) and 6(b), (c) that the thermal stress in aluminum plate can be calculated by Eq.(9). Further, the stress in aluminum

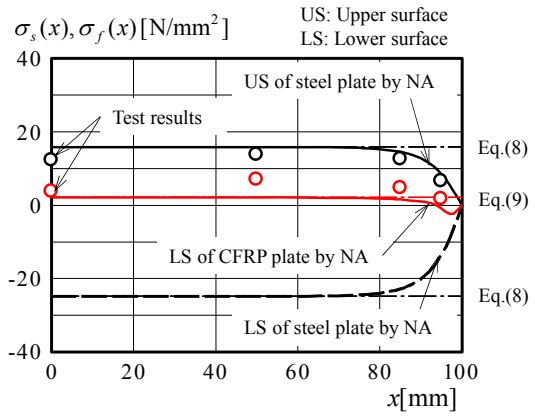


(a) Specimen CC

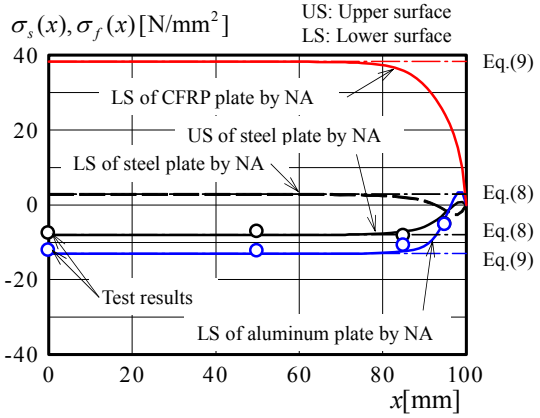


(b) Specimen CA

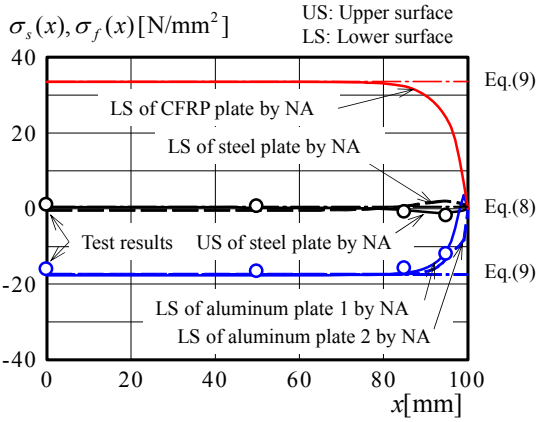


(c) Specimen ACA

Figure 5. Stress distribution (4.5mm steel plate)

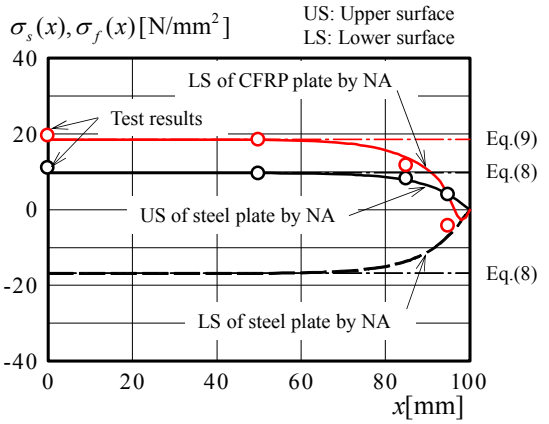


(a) Specimen CC

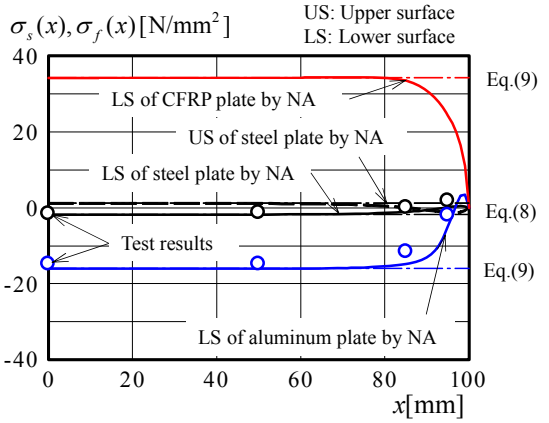


(b) Specimen CA

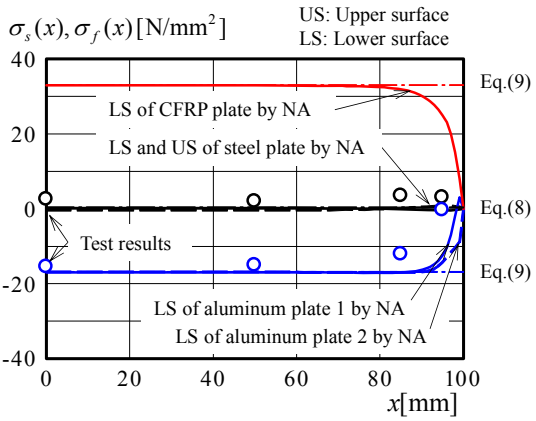


(c) Specimen ACA

Figure 6. Stress distirbution (12mm steel plate)

plate under loading is calculated by using composite theory. Therefore, a structural aluminum alloy should be used for the laminated plate. Note that the stress in aluminum plate is relatively smaller than steel member, because the Young's modulus of aluminum alloy is one third of that of steel even though the strains in steel member and aluminum plate are almost same in the interface of them.

**Thermal stresses induced in adhesive layers**

From the test results, the shear stress in adhesive layer 1 can be calculated by the following equation.

$$\tau_{e1}\left(\frac{L_{k+1}+L_k}{2}\right)=-\frac{E_s A_s}{b_1}\cdot\frac{\varepsilon_{Ns}(L_{k+1})-\varepsilon_{Ns}(L_k)}{L_{k+1}-L_k} \tag{29}$$

where, $L_k$ is the distance from the center of the specimen to the location of the strain gage $k$, $\varepsilon_{Ns}(L_k)$ is the

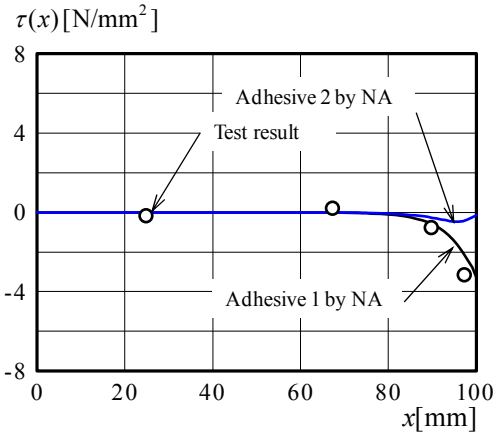


(a) Specimen CC

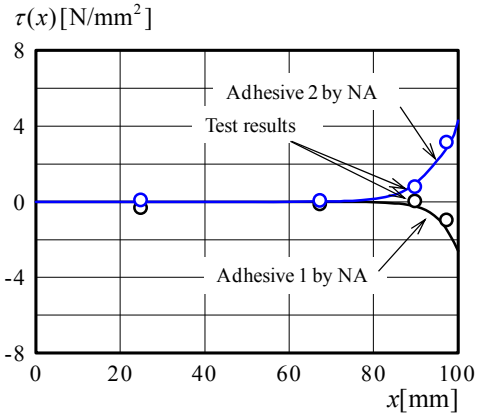


(b) Specimen CA

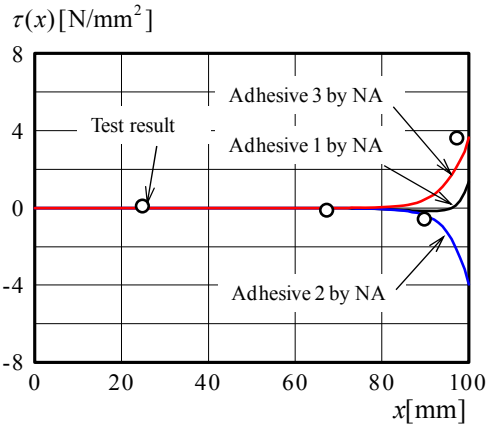


(c) Specimen ACA

Figure 7. Shear stress distribution (4.5mm steel plate)

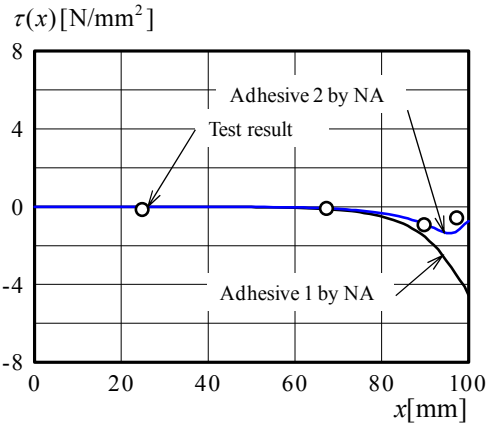


(a) Specimen CC

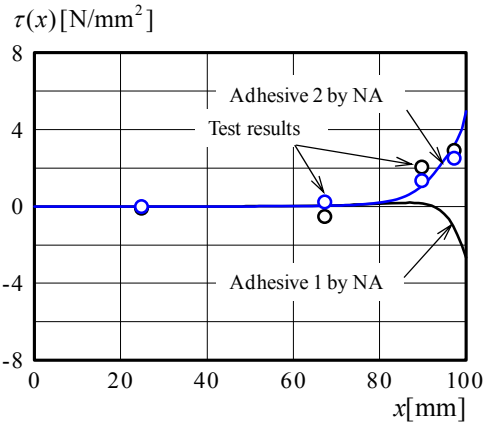


(b) Specimen CA

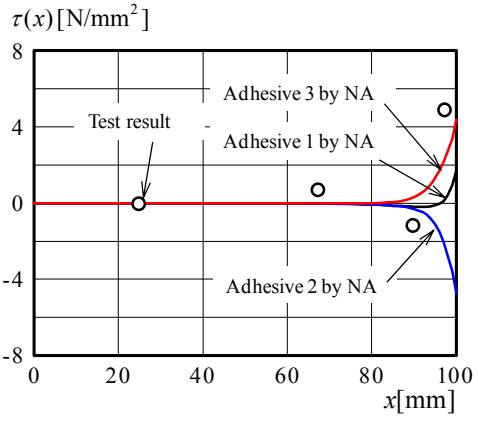


(c) Specimen ACA

Figure 8. Shear stress distribution (12mm steel plate)

axial strain introduced in steel plate at $L_k$ and $b_1$ is the bond width of plate 1.
The axial strains in steel plate can be measured by mounting the strain gages onto the side edge with mid-thickness of the steel plate.
As the same way, the shear stress in adhesive layer 2 also can be calculated with the following equation.

$$\tau_{e2}\left(\frac{L_{k+1}+L_k}{2}\right)=\frac{E_2A_2}{b_2}\cdot\frac{\varepsilon_{N2}(L_{k+1})-\varepsilon_{N2}(L_k)}{L_{k+1}-L_k} \tag{30}$$

where, $\varepsilon_{N2}(L_k)$ is the axial strains in plate 2 at $L_k$ and $b_2$ is the bond width of plate 2 ( $b_1 \geq b_2$ ).
In this study, for the calculation of shear stress in adhesive layer 2, it was only possible to measure the axial strains of aluminum plate of 2mm in specimen CA, because the 1mm in thickness of CFRP and aluminum plate are not enough to mount the strain gages.
The shear stresses introduced in the adhesive layers calculated by the test results are shown in Figs.7 and 8. In these figures, Y-axis shows the shear stress in adhesive layers. It can be seen from Fig.7 that the shear stresses of NA in all specimens are close agreement with the test results. However, the test results in Fig.8 are not plotted on the NA curves, the reason of this is depending on the accuracy of the location of strain gages.
In Figs.7 and 8, the shear stresses at the end of adhesive layer 1 in specimens CA and ACA become smaller than that in specimen CC. However, the shear stresses in adhesive layer 2 in specimens CA and ACA become higher than that in specimen CC. Therefore, in proposed method, it might be concerned about the debonding at the adhesive layer 2.

## CONCLUSIONS

In this study, to confirm the reduction of thermal stress in steel plate by using the laminated plate consisted of CFRP and aluminum plates, heat tests of steel plate with laminated plate on one side were carried out. Additionally, to verify the test results, a numerical analysis was proposed and carried out. The main conclusions are as follows;

(1) The required cross-sectional areas of CFRP and aluminum alloy plates for proposed method are designed by using Eqs.(3) and (4).
(2) It was found that the use of laminated plate consisted of CFRP and aluminum plates is effective to reduce the thermal stress in steel plate. Furthermore, the odd-layers of laminated plate is required for completely reduction of thermal stress in thin steel plate with laminated plate.
(3) The thermal stresses introduced in CFRP and aluminum alloy plates can be estimated by Eqs.(8) and (9), respectively.
(4) Distribution of thermal stresses in steel plate strengthened by bonding laminated plate on one side can be demonstrated by using numerical analysis proposed in this study.

## ACKNOWLEDGMENTS

The authors gratefully acknowledge the financial support provided by JSPS Grant-in-Aid for challenging Exploratory Research (24656269).

## APPENDIX

The submatrix in matrix *A* are:

$$\underset{3\times3}{B_0}=\begin{bmatrix}0&0&0\\0&0&0\\0&0&0\end{bmatrix},\ \underset{3\times3}{B_1}=\begin{bmatrix}0&0&1\\0&0&0\\0&0&0\end{bmatrix},\ \underset{3\times3}{B_{ai}}=\begin{bmatrix}0&0&0\\0&0&0\\0&\dfrac{G_iA_i'd_i}{E_iI_i}&0\end{bmatrix},\ \underset{3\times3}{B_{bi}}=\begin{bmatrix}0&\dfrac{-G_{ei}b_i}{E_{i-1}A_{i-1}}&0\\\dfrac{-E_{ei}b_i}{G_{i-1}A_{i-1}'}&0&0\\0&\dfrac{-G_{ei}b_id_{i-1}}{E_{i-1}I_{i-1}}(d_{i-1}+\dfrac{h_i}{2})&0\end{bmatrix},$$

$$\underset{3\times3}{B_{ci}}=\begin{bmatrix}0&\dfrac{G_{ei}b_i}{E_iA_i}&0\\\dfrac{E_{ei}b_i}{G_iA_i'}&0&0\\0&\dfrac{-G_{ei}b_id_i}{E_iI_i}(d_i+\dfrac{h_i}{2})&0\end{bmatrix},\ \underset{3\times3}{B_{di}}=\begin{bmatrix}0&0&0\\-\dfrac{1}{h_i}&0&-\dfrac{d_{i-1}+h_i/2}{h_id_{i-1}}\\0&0&\dfrac{1}{h_id_{i-1}}\end{bmatrix},\ \underset{3\times3}{B_{ei}}=\begin{bmatrix}0&0&0\\\dfrac{1}{h_i}&0&-\dfrac{d_i+h_i/2}{h_id_i}\\0&0&-\dfrac{1}{h_id_i}\end{bmatrix}$$

**REFERENCES**


Ishikawa, T., Hattori, A. and Kawano, H. (2011) “Reduction of thermal stress induced in CFRP bonded steel plate by additionally bonding of aluminum alloy plates”, *Journal of Japan Society of Civil Engineers, Ser. A1 (Structural Engineering & Earthquake Engineering (SE/EE))*, Vol.67, No.2, pp.336-350 (in Japanese)

Ishikawa, T., Hattori, A., Kawano, H., Nagao, T. and Kobayashi, A. (2012) “Development of reduction technique of thermal stress Induced in CFRP bonded steel plates”, Asia-Pacific Conference on FRP in Structures, APFIS, Sapporo, Japan, Paper No. F2B04

Miller, T. C., Chajes, M. J., Mertz, D. R. and Hastings, J. N. (2001) “Strengthening of a steel bridge girder using CFRP plates”, *Journal of Bridge Engineering*, ASCE, Vol.6, pp.514-522, 2001

Miyashita, T. and Nagai, M. (2010) “Stress analysis for plate with multilayered CFRP under uni-axial loading”, *Doboku Gakkai Ronbunshuu A*, Vol.66, No.2, pp.378-392 (in Japanese)

Moy, S. S. J. and Bloodworth, A. G. (2007) “Strengthening a steel bridge with CFRP composites”, *Structures & Buildings*, Vol.160, Issue SB2, pp.81-93

National Research Council - Advisory Committee on Technical Recommendations for Construction (2007) “Guidelines for the Design and Construction of Externally Bonded FRP Systems for Strengthening Existing Structures”, CNR-DT 202/2005

Schnerch, D., Dawood, M., Rizkalla, S. and Sumner, E. (2007) “Proposed design guidelines for strengthening of steel bridges with FRP materials”, *Construction and Building Materials*, Vol.21, pp.1001-1010

Täljsten B., Hansen C.S. and Schmidt J.W. (2009) Strengthening of old metallic structures in fatigue with prestressed and non-prestressed CFRP laminates, *Construction and Building Materials*, Vol.23, 1665–1677.

Tamai, H., Takamatsu, T., Hattori, A., Haitani, T. and Sakuraba, M. (2005) “Rehabilitation of secondary beam in chemical plant frame using carbon fiber reinforced plastic plate”, *Journal of Construction Steel*, JSSC, Vol.13, pp.545-552 (in Japanese)